INFERRING SOIL SURFACE ROUGHNESS FROM SOIL BIDIRECTIONAL REFLECTANCE DATA

J. Cierniewski[1], *M. Verbrugghe*[2]

[1]Institute of Physical Geography, Adam Mickiewicz University, Fredry 10, 61-701 Poznań, Poland
[2]I.N.R.A. Bioclimatologie, Site Agroparc,84914 Avignon cedex 9, France

A b s t r a c t. This work is an attempt to assess the accuracy of soil surface roughness estimations based on analysis by inverse model of bidirectional soil reflectance data.

K e y w o r d s: soil bidirectional reflectance, visible and near infrared, soil surface roughness, invertion model.

INTRODUCTION

Rough soil surfaces, as most natural objects, show in brightness variations caused by direction of irradiation and also the direction from which reflectance is measured. In the absence of strong specular behaviour, a soil surface seems to be brightest from the direction which gives the lowest proportion of shaded fragments. That soil surface usually displays a clear backscattering character with a reflectance peak towards the Sun position ('hot spot' direction), and decreasing reflectance in the direction away from the peak, with minimum reflectance in the extreme forward scatter direction near the horizon [12,13,15]. The hot spot tends to be more pronounced when solar zenith angle increases. Soil reflectance could also have a forward scattering character due to specular reflection as observed on an alkali flat bare soil and on a flat gypsum sand surface with uniform ripples [9].

The non-Lambertian behaviour of a soil surface depends on its roughness at micro-scale and larger scales, as well as on the incident angle of the direct solar beam on the surface. If the surface in micro-scale is smooth in relation to the wavelength, the sunbeams are reflected specularly in a directional way, where the angle of incidence equals the angle of reflection. If the soil surface in the scale is rough, the sunbeam energy falling on the surface is dispersed into vectors creating the ideal shape of a sphere, independent of the angle of incidence. The criterion of roughness to divide between smooth and rough particle surfaces in micro-scale depends on wavelength and the incidence angle of the direct solar beam. For the visible and near-infrared range and for incidence angles from $10°$ to $70°$, the critical height variation of the surface according to Rayleigh's formula is between $0.05 \mu m$ and $0.47 \mu m$ [4]. Irregularities of a soil's surface at larger scales, caused by soil aggregates and clods, make it impossible to illuminate the whole surface directly. These elements produce shadow on soil surface fragments. Energy reflected from these fragments is many times lower than energy leaving sunlit soil fragments and it becomes another important factor influencing the non-Lambertian distribution of the soil re-radiation [10,11,16,17]. The degree of soil surface shadowing depends on the density of the elements casting shadow,

the general configuration of the soil surface and its slope in relation to incident rays.

Geometrical soil directional reflectance models, describing a soil surface as a plane varying periodically with cosine [8], simulating soil aggregates as cuboids [14], spheres [1,2], or spheroids, [5,6], regularly spaced predict soil bidirectional reflectance based on the assumption that shadowing of soil surface has a greater influence than the scattering properties of a soil material at micro-scale. All the models assume only perfectly diffuse reflection from directly illuminated soil fragments. Improved versions of the last mentioned model [3,7] take into account the diffuse as the specular component of energy leaving soil surface in the visible and near-infrared.

In the work presented the authors try to answer how precisely it is possible to infer about soil surface roughness from soil bidirectional reflectance data using an inversion of the soil reflectance model incorporating specular effects [7].

METHODS

The model

The model predicts the reflectance distribution of a horizontal soil surface along the solar principal plane. Equal-sized spheroids of horizontal (a) and vertical (b) radii lying on a flat horizontal surface simulate the soil surface. They are regularly spaced at a distance 'd'. The spheroids are given as composites of small planar units. The geometrical structure is illuminated by the direct solar beam at a zenith angle θ_s, and diffuse skylight, defined by the ratio of its energy to direct light (f_{di}) (Fig. 1).

The model calculates the area of illuminated and shaded fragments of the simulated soil surface, visible at a given view zenith angle (θ_v) of the sensor, and then the electromagnetic energy coming to each facet of the structure. The slope angle of each facet (β) and its azimuth angle (ϕ_r), together with the solar zenith (θ_s) and azimuth (ϕ_s) angles, determine the amount of energy reaching the sunlit surface using the factor (E_{fa}), defined as:
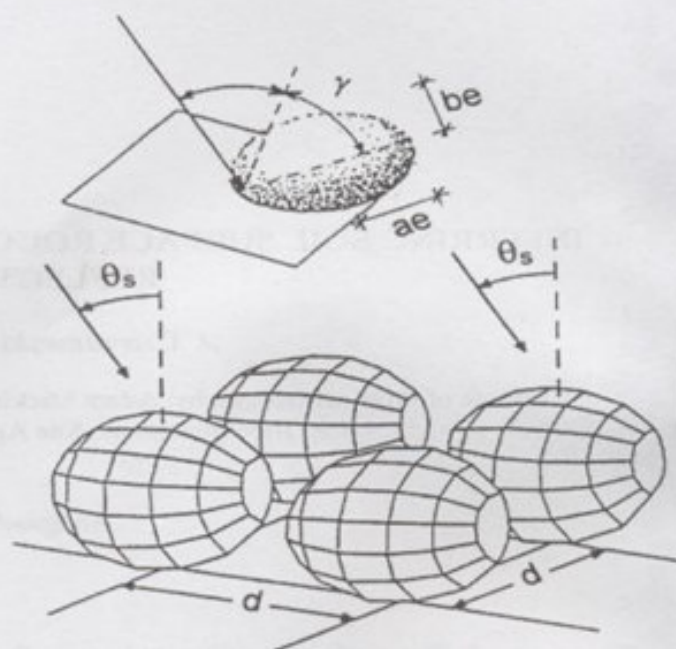

Fig. 1. Geometry of simulated soil surface and distribution of vectors of the near-perfect specular component of energy leaving one facet of the surface, where ae and be are the major and minor radius of the first component, g is the angle of the reflected sunbeams to the normal and θs is the solar zenith angle.

$$E_{fa} = \cos\theta_s \cos\beta +$$
$$\sin\beta \sin\theta_s (\sin\phi_s \sin\phi_r + \cos\phi_s \cos\phi_r) \quad (1)$$

This factor express the cosine of the incidence angle (γ) of the direct solar beam to the facet. A part of the direct energy is reflected as from a near-perfect specular object and a part as from a perfect diffuse one.

Energy reflected in the near-perfect specular way is dispersed into vectors (v_{sp}) creating an spheroidal shape of elongation (el) depending on the intensity of polarization ($Fp_{(\gamma)}$) of the reflected energy E_{fa} at the γ angle, as:

$$el = ae/e = 1/(1 - Fp_{(\gamma)}) = r_\perp^2 - r_=^2, \quad (2)$$

where ae and be are the major and minor radius of the spheroid, and $r_\perp$ and $r_=$ are respectively the perpendicular and parallel Frasnel reflection coefficient, given by:

$$r_\perp = (n\mu_T - \mu_I)/(n\mu_T + \mu_I)$$

and

$$r_= = (n\mu_I - \mu_T)/(n\mu_I + \mu_T)$$

with $\mu_1 = \cos\gamma = E_{fa}$

and $\mu_T = (1 - \sin^2\gamma / n^2)^{0.5}$ \hfill (3)

where n is the refractive index of the reflective medium.

Energy leaving a given facet in the perfectly diffuse way is dispersed into equal-size vectors (v_{di}) creating the ideal shape of sphere.

The proportion between the near-perfect specular and the perfect diffuse energy expresses the specular-diffuse coefficient (SDC), defined as:

$$SDC = V_{sp} / V_{di} \hfill (4)$$

where V_{sp} and V_{di} are respectively volume of the v_{sp} vectors spheroid, and the v_{di} vectors of the sphere.

The energy outgoing from a given sunlit facet (Ei_{fa}), sensed by the sensor from the given direction (θ_v), is defined as:

$$Ei_{fa} = E_{fa}[SDC^{1/3}v_{sp} +$$

$$(1 - SDC^{1/3})v_{di}] + f_{di} \hfill (5)$$

where f_{di} is the ratio of skylight to direct light for the given wavelength, is proportional to the area of a given sunlit facet (Ai_{fa}). The energy leaving the shaded facet (Es_{fa}), expressed by the f_{di} fraction of anisotropic distribution, is proportional to the area of shaded facet (As_{fa}). The relative radiance of the simulated field surface ($L_{(qv)}$) visible to the radiometer from the given direction (θ_v) can be formulated as:

$$L_{(\theta v)} = \frac{\sum\limits_{i=1}^{j} Ei_{fai}Ai_{fai} + \sum\limits_{i=1}^{j} Es_{fai}As_{fai}}{\sum\limits_{i=1}^{j} Ai_{fai} + As_{fai}} \hfill (6)$$

where i is i^{th} facet of the geometrical structure visible inside of the field-of-view of the radiometer at angle θ_v.

The reflectance of the simulated surface is finally expressed by the relative reflectance factor (RRF), which is defined as the ratio of the total radiance measured from the off-nadir direction to the radiance measured from nadir.

Observed data

Validation of the model to inferring about soil surface roughness were tested using soil bidirectional reflectance data acquired on a bare field on the alluvial plain covered by pebbles of several centimetres diameter (Fig. 2) of the Rhöne river, named La Crau, located 40 km to the south of Avignon, and 15 km north of the Mediterranean Sea in southern France.

Reflectance data of the field were measured by a three-channel (XS1:0.50-0.59 μm, XS2: 0.61-0.68 μm and XS3: 0.79-0.89 μm) field radiometer CIMEL simulating the SPOT (HRV) bands. It collected radiance data along the solar principal plane in 13 directions at view zenith angles from 60° towards the Sun through the nadir to 60° back from the Sun at 10° increments. The radiometer observed the soil surface from a distance of 2 m, inside of its 12° field of view.

Simultaneously to the radiometer data collecting, photographs of the target, viewed by the radiometer, were taken. The photographs were used to assess roughness parameters of the soil surface.

RESULTS AND DISCUSSION

The soil roughness is described in the model by three parameters: the b/a ratio defining the flatness of the spheroids simulating the soil pebbles, the relative distance between the spheroids (d/a), and the specular-diffuse coefficient (SDC) characterising optical properties of the soil material. Values of these parameters were determined by a simple optimisation technique, separately for each series of measured reflectance data referring to the given illumination conditions defined by the solar zenith angle (θ_s) and the skylight ratio f_{di} for the three radiometer channels. We computed the distance between the measured BRDF and the values simulated for a range of: b/a from 0.2 to 1 at 0.05 increments, d/a from 2.1 to 2.8 at 0.05 increments, and SDC from 0 to 0.16 at 0.02 increments. These values of the b/a, d/a, and SDC which provide the lowest root mean square error were selected as the result of the model

Fig. 2. Photography of the tested soil surface and the geometrical structure, being the result of the geometrical model inversion, used in the paper.

inversion, i.e., as the parameters which characterise the tested soil surface in the best way.

The soil surface roughness parameters the best fitted to measured bidirectional reflectance data are presented in Table 1. Values of the specular-diffuse coefficient (SDC) of the tested soil material are constant for all the analysed illumination conditions, but values of the relative distance between soil pebbles (d/a) and their flatness (b/a) progressively vary with illumination conditions changing. The variation of the d/a, contained between 2.25 and 2.45 is not so strong as the variation of the b/a, reaching the range from 0.4 to 0.7.

A reason for this variation is probably a result of a divergence of geometrical assumption of the model from real geometry of the tested soil surface. The model assumes that simulated soil aggregates, clods or pebbles, have only a spheroidal shape and are equal-sized and regularly spaced on a flat surface. In fact the real pebbles are heterogeneous in their rounded shape in their horizontal projection, their flatness, and their distance from one another. The diameter of the tested soil surface pebbles varies from about 1.5 cm to 10 cm and their flatness from about 0.3 to 0.9 (Fig. 3). The heterogeneity of the shape of the natural

pebbles produces an heterogeneity of relation between the pebbles and the illumination conditions. It is demonstrated on 20 selected pebbles lying inside of the radiometer field of view, illuminated at four different Sun positions (Fig. 4). Measuring relative length shadow of the pebbles on the ground (x_{sh}/a) at the given solar zenith angle, we determined the value of the flatness of the pebbles (b/a) which corresponds to the x_{sh}/a with assumption that all of them are ideal spheroids (Table 2). The following equations were used for this procedure (Fig. 4):

$$x_{sun} = [\tan(90-\theta_s)]/[\tan^2(90-\theta_s)+$$
$$(b/a)^2]^{1/2};$$

$$y_{sun} = ba^2 x_{sun}/\tan(90-\theta_s)-b/a \qquad (7)$$

$$x_{sh} = x_{sun} + \tan\theta_s(y_{sun}+2b/a). \qquad (8)$$

If we describe the roughness of the tested soil surface as the mean values of the b/a and d/a from all the values obtained as the results of the model inversion, it could be characterised by the flatness $b/a = 0.55$ and the relative distance between pebbles $d/a = 2.35$. These mean values are very close to results of

T a b l e 1. Results of the geometrical model inversion, describing flatness of the pebbles (b/a) and their relative spacing (d/a), and statistical parameters, coefficient of determination (r^2) and root mean square (rms) error characterizing fitting of the simulated soil surface reflectance to the measured reflectance data for given illumination, expressed by the solar zenith angle (θ_s), solar azimuth angle (ϕ_s), and the ratio between diffuse and direct energy (f_{di}) coming to the measured soil surface for three radiometer channel: XS1, XS2 and XS3

| | | f_{di} | | | | | XS1 | | XS2 | | XS3 | |
ϕ_s (°)	θ_s (°)	XS1	XS2	XS3	b/a	d/a	r^2	rms	r^2	rms	r^2	rms
90.2	62.5	0.401	0.321	0.262	0.40	2.45	0.956	0.052	0.936	0.093	0.924	0.092
98.5	54.1	0.351	0.289	0.235	0.40	2.45	0.923	0.104	0.964	0.113	0.965	0.093
105.2	48.3	0.322	0.265	0.217	0.50	2.40	0.969	0.066	0.976	0.078	0.948	0.073
114.8	41.3	0.302	0.251	0.207	0.60	2.35	0.967	0.059	0.971	0.050	0.954	0.064
123.2	36.5	0.276	0.226	0.182	0.65	2.25	0.969	0.064	0.979	0.057	0.954	0.071
135.2	31.6	0.281	0.226	0.180	0.70	2.25	0.914	0.099	0.954	0.061	0.900	0.090
150.1	27.7	0.263	0.211	0.174	0.70	2.25	0.960	0.060	0.967	0.053	0.957	0.044
174.0	25.2	0.254	0.200	0.163	0.70	2.25	0.954	0.048	0.941	0.049	0.949	0.035
192.4	25.5	0.251	0.197	0.161	0.70	2.35	0.956	0.048	0.936	0.056	0.940	0.047
214.8	28.8	0.258	0.204	0.166	0.65	2.35	0.946	0.051	0.959	0.047	0.965	0.036
230.5	33.7	0.250	0.200	0.165	0.50	2.35	0.922	0.061	0.909	0.059	0.919	0.048
243.8	40.3	0.252	0.208	0.174	0.45	2.35	0.912	0.071	0.934	0.059	0.917	0.071
253.0	46.8	0.271	0.221	0.184	0.45	2.35	0.945	0.077	0.956	0.083	0.932	0.066
264.8	57.3	0.324	0.272	0.226	0.40	2.45	0.920	0.082	0.925	0.108	0.945	0.091
266.8	66.0	0.372	0.307	0.256	0.40	2.45	0.963	0.096	0.952	0.086	0.942	0.090
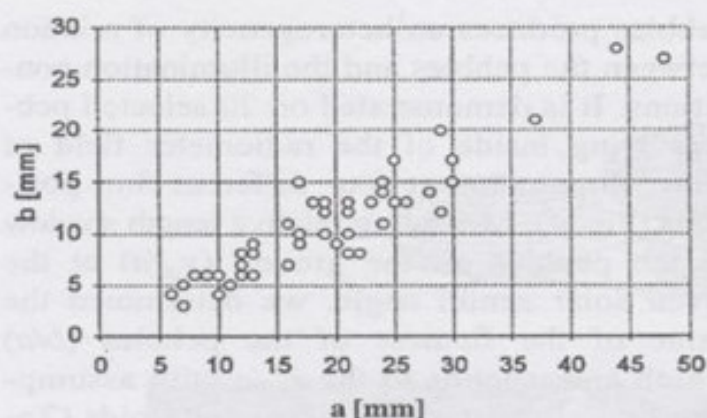
Fig. 3. Shape of pebbles situated inside of the radiometer field of view at the nadir ($\theta v = 0$), characterised by their horizontal (a) and vertical (b) radii.

another geometrical model test, carried out on the same soil surface [5]. The b/a and d/a values were determined in this previous test as 0.56 and 2.37, respectively.

Satisfying results of soil surface geometry reconstruction, expressed by the fact that that the soil surface generated by the model is close to the real shape, are probably due to quite simple geometry of the tested surface. Typical cultivated soil surfaces are geometrically more

complicated, especially, soil surface developed from heavy texture materials which create porous aggregates with necessarily rounded edges. They could not be described precisely enough by models simulating them by equal-sized spheroids. Thus, the inversion of this model used as the method for inferring about soil surface roughness from soil bidirectional reflectance data probably is limited to soil surfaces containing simple dense particles of rounded edges not creating secondary aggregates.

The soil surface roughness parameters, obtained as the result of the inversion of the model presented in this paper, were fitted to each of the analysed illumination conditions with the similar accuracy level (Fig. 5, Table 1). A linear regression analysis has been performed between the relative reflectance factor (RRF) of measured data and data resulting from inversion modelling. For the three channels we found values of coefficient of determination (r^2) between 0.9 and 0.92, and mean deviation (rms) error of about 0.06 - 0.062

T a b l e 2. Flatness of pebbles (b/a) determined from the relative distance of the shadow boundary on the ground (x_{sh}/a) in relation to the center of a given pebble for chosen solar zenith (θ_s) and azimuth (ϕ_s) angles. The b/a values are calculated with the assumption that the pebbles have a spheroid shape

Pebble no.	$\phi_s=105.2°$; $\theta_s=48.3°$		$\phi_s=114.8°$; $\theta_s=41.3°$		$\phi_s=135.2°$; $\theta_s=31.6°$		$\phi_s=264.8°$; $\theta_s=57.3°$	
	x_{sh}/a	b/a	x_{sh}/a	b/a	x_{sh}/a	b/a	x_{sh}/a	b/a
1	1.92	0.64	1.67	0.57	1.40	0.60	1.92	0.47
2	-	-	-	-	1.40	0.60	1.83	0.42
3	-	-	1.71	0.62	1.50	0.67	1.88	0.47
4	2.00	0.60	1.67	0.57	1.60	0.76	-	-
5	1.80	0.56	1.60	0.56	1.50	0.70	-	-
6	1.80	0.56	-	-	-	-	1.43	0.25
7	1.67	0.40	1.50	0.47	1.60	0.72	1.80	0.45
8	1.60	0.42	1.71	0.60	1.44	0.60	-	-
9	1.71	0.45	-	-	-	-	1.89	0.45
10	1.71	0.45	1.71	0.60	1.43	0.60	-	-
11	1.60	0.43	1.80	0.75	1.50	0.67	1.67	0.34
12	-	-	1.71	0.60	1.50	0.70	-	-
13	1.86	0.60	-	-	1.57	0.75	1.86	0.46
14	-	-	1.67	0.57	-	-	2.00	0.47
15	-	-	-	-	1.50	0.67	1.57	0.30
16	-	-	-	-	1.56	0.75	1.40	0.22
17	1.60	0.43	-	-	-	-	1.80	0.45
18	-	-	1.67	0.57	1.44	0.60	1.62	0.32
19	1.67	0.47	-	-	1.50	0.67	1.83	0.42
20	1.60	0.43	1.60	0.50	1.50	0.67	-	-

$\phi_s = 105.2°$
$\theta_s = 48.3°$

$\phi_s = 135.2°$
$\theta_s = 31.6°$

$\phi_s = 114.8°$
$\theta_s = 41.3°$

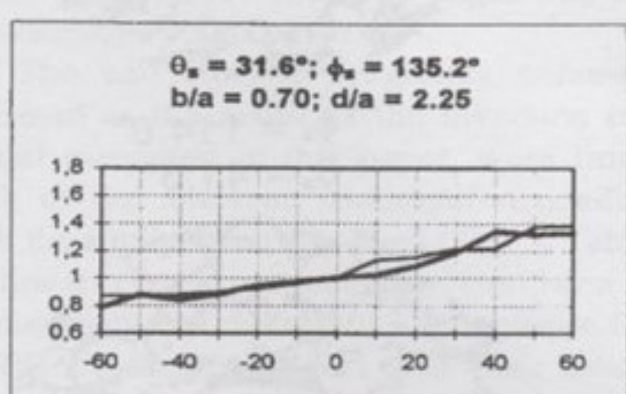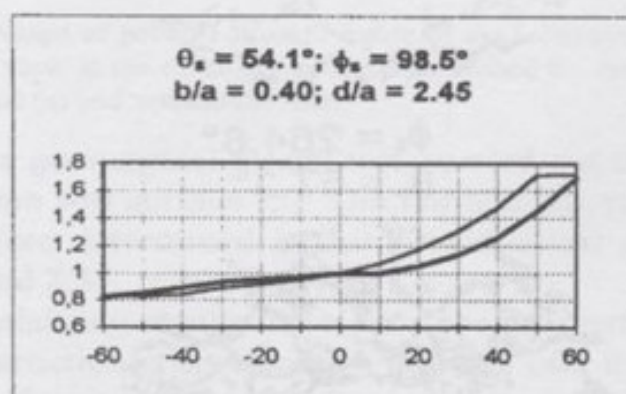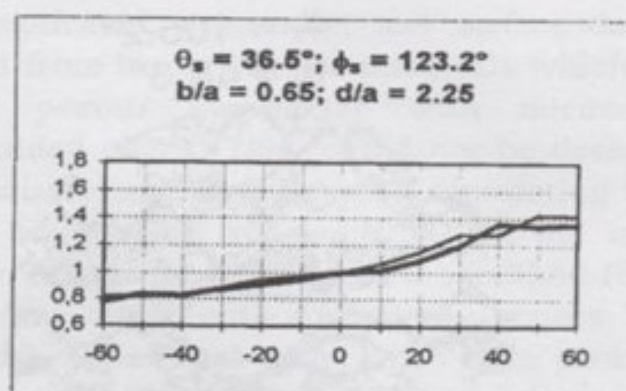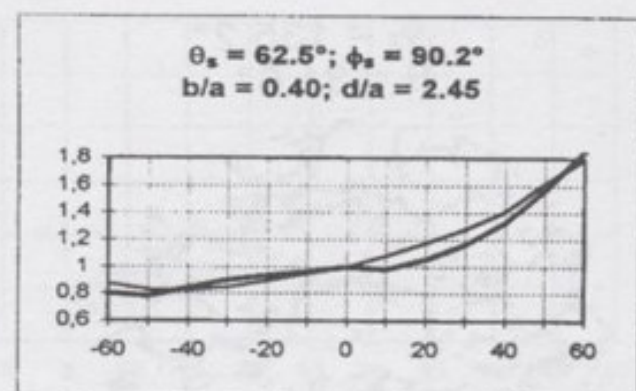$\phi_s = 264.8°$
$\theta_s = 57.3°$
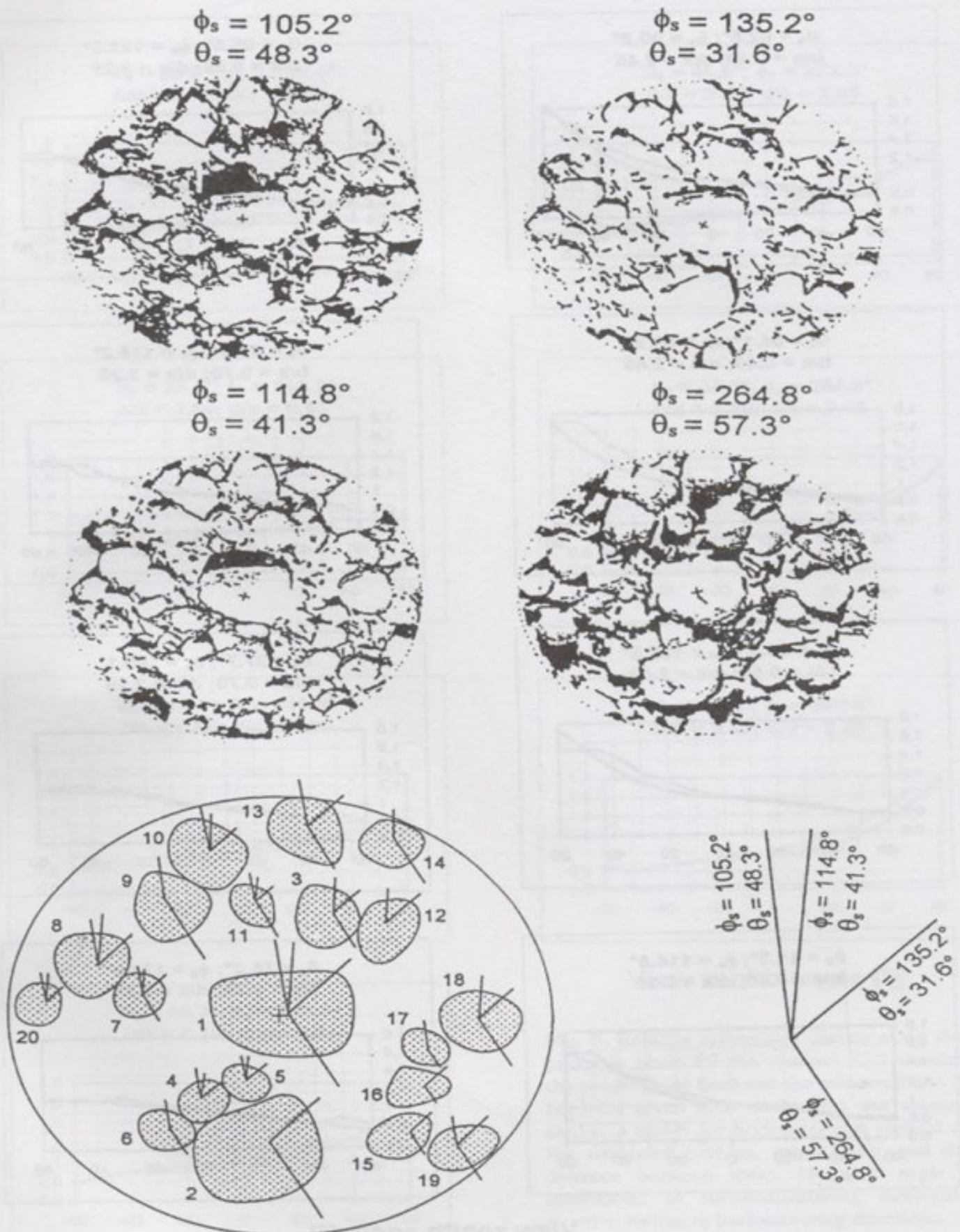
Fig. 4. Length of selected pebbles shadows inside of the radiometer field of view, viewed the tested soil surface at the nadir ($\theta_v = 0$), illuminated at four the Sun position, defined by the solar zenith θ_s and azimuth ϕ_s angles.

Relative reflectance factor

$\theta_s = 62.5°$; $\phi_s = 90.2°$
$b/a = 0.40$; $d/a = 2.45$

$\theta_s = 36.5°$; $\phi_s = 123.2°$
$b/a = 0.65$; $d/a = 2.25$

$\theta_s = 54.1°$; $\phi_s = 98.5°$
$b/a = 0.40$; $d/a = 2.45$

$\theta_s = 31.6°$; $\phi_s = 135.2°$
$b/a = 0.70$; $d/a = 2.25$

$\theta_s = 48.3°$; $\phi_s = 105.2°$
$b/a = 0.50$; $d/a = 2.40$

$\theta_s = 27.7°$; $\phi_s = 150.1°$
$b/a = 0.70$; $d/a = 2.25$

$\theta_s = 41.3°$; $\phi_s = 114.8°$
$b/a = 0.60$; $d/a = 2.35$

$\theta_s = 25.2°$; $\phi_s = 174.0°$
$b/a = 0.70$; $d/a = 2.25$
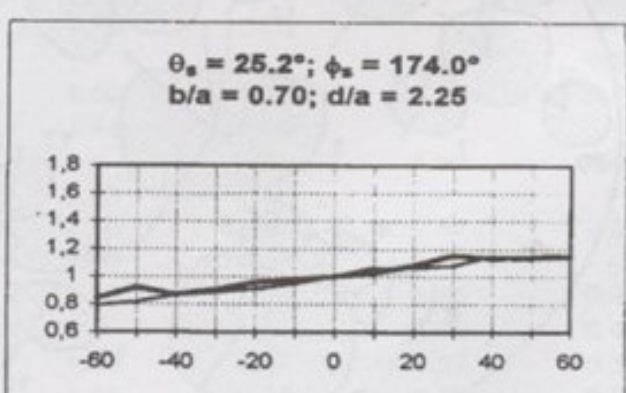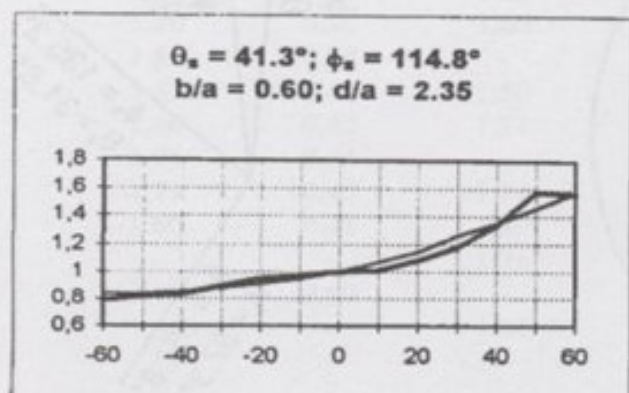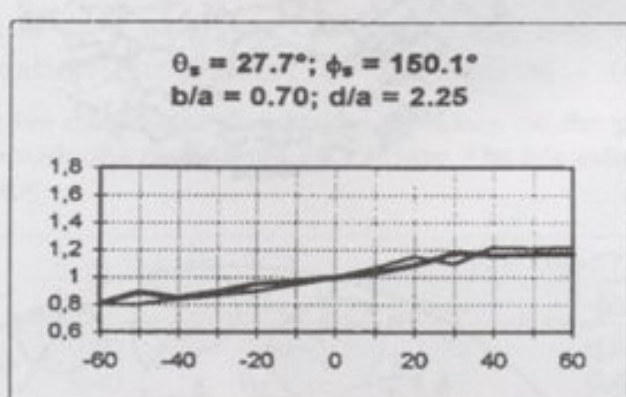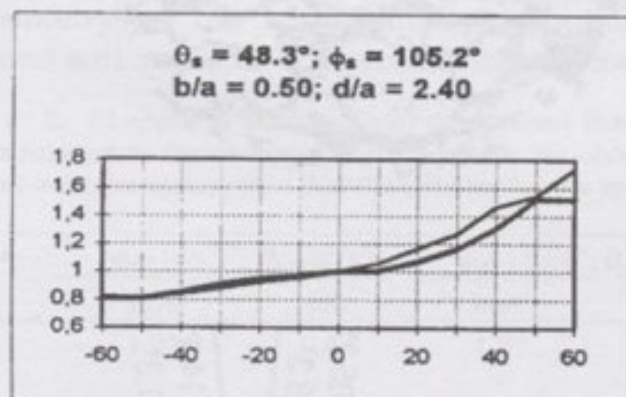
View zenith angle [°]

Fig. 5. See next page.

Relative reflectance factor

$\theta_s = 25.5°; \phi_s = 192.4°$
$b/a = 0.70; d/a = 2.35$

$\theta_s = 46.8°; \phi_s = 253.0°$
$b/a = 0.45; d/a = 2.35$

$\theta_s = 28.8°; \phi_s = 214.8°$
$b/a = 0.65; d/a = 0.65$

$\theta_s = 57.3°; \phi_s = 264.8°$
$b/a = 0.40; d/a = 2.45$

$\theta_s = 33.7°; \phi_s = 230.5°$
$b/a = 0.50; d/a = 2.35$

$\theta_s = 66.0°; \phi_s = 266.8°$
$b/a = 0.40; d/a = 2.45$

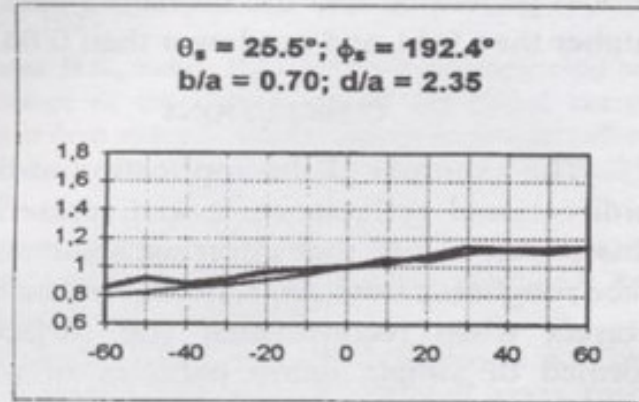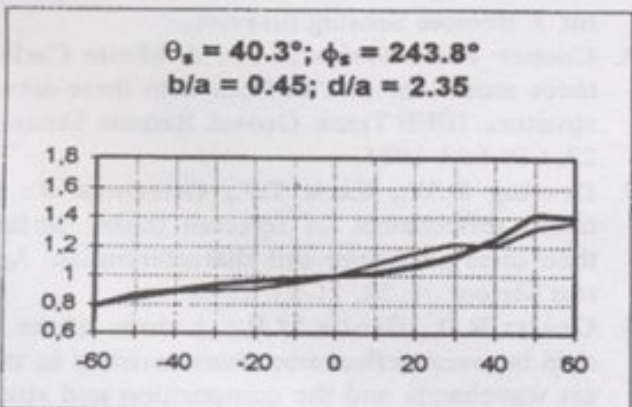$\theta_s = 40.3°; \phi_s = 243.8°$
$b/a = 0.45; d/a = 2.35$
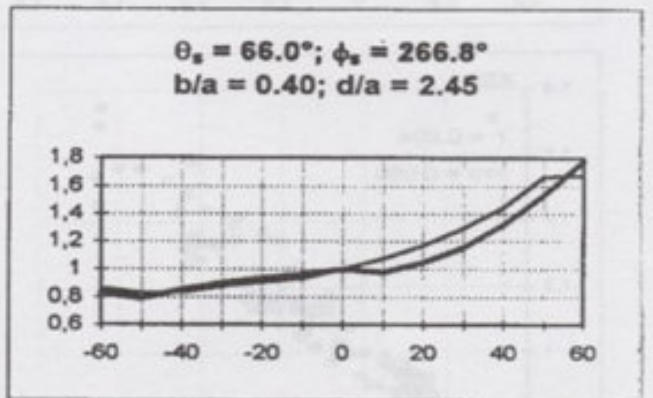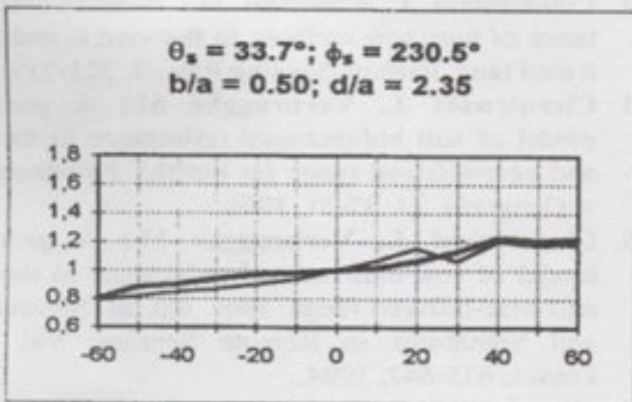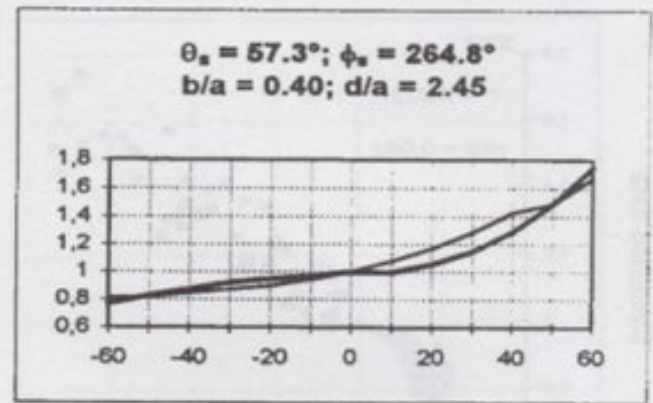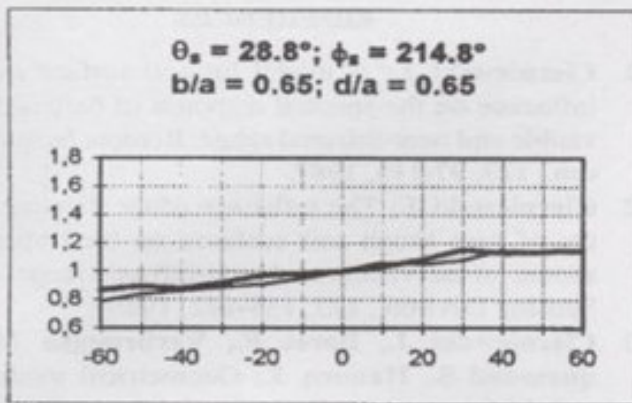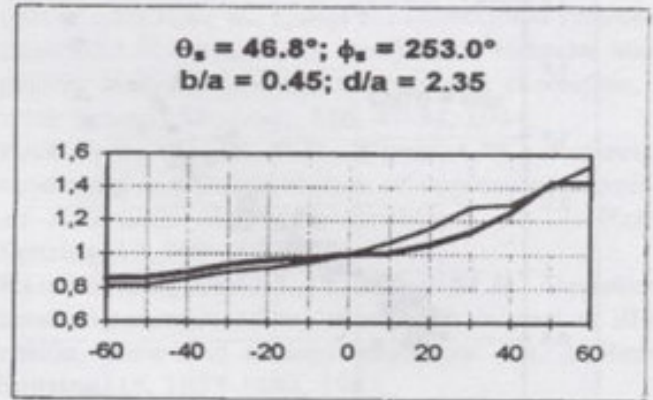
View zenith angle [°]

Fig. 5. Relative reflectance curves along the solar principle plane for the channel XS2 simulated by the model (bold line) and the measured one (simple line) for given solar zenith (θ_s) and azimuth (ϕ_s) angles. a and b are horizontal and vertical radii of the simulated pebbles, respectively, and d is the distance between them. Negative angle values correspond to forwardscattering directions, but positive values, to backscattering directions.
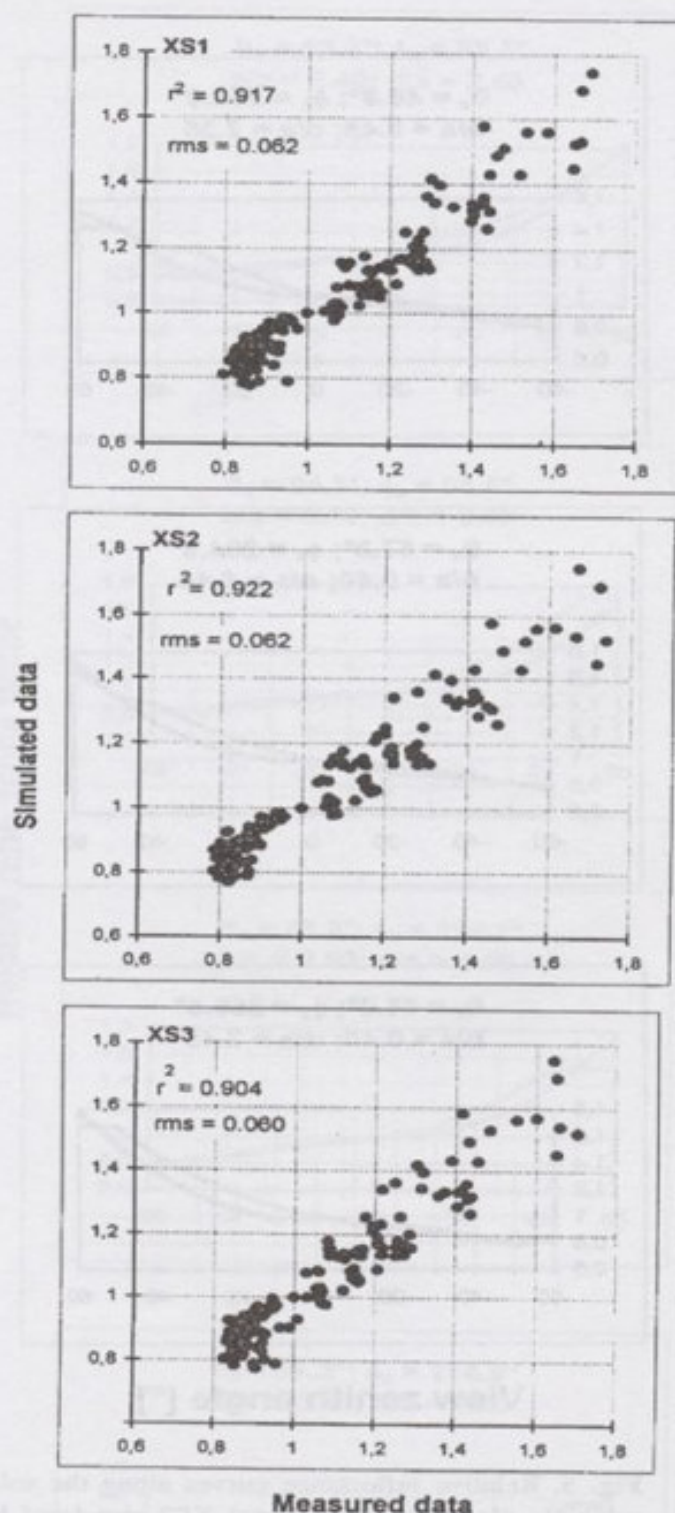
Fig. 6. Relationship between measured and simulated soil relative reflectance factor (RRF) of analysed soil surface for XS1, XS2 and XS3 channels of the radiometer. r^2 is the coefficient of determination, and rms is the root mean square error of the analysed pairs of data.

(Fig. 6). The r^2 and rms, computed separately for each of the analysed illumination conditions, presented in Table 1, indicate that the goodness-off-fit is between 90 and 98 %.

The relative root mean square error between model generated and the measured data is not higher than 0.11 and not lower than 0.04.

CONCLUSIONS

The example of the application of the soil bidirectional reflectance model, presented in this paper, shows that inferring about soil surface roughness from soil reflectance data is quite correct when reconstructed soil surfaces are formed of simple dense particles of rounded edges not creating secondary aggregates.

REFERENCES

1. **Cierniewski J.:** A model for soil surface roughness influence on the spectral response of bare soils in the visible and near-infrared range. Remote Sensing Environ., 123, 97-115, 1987.
2. **Cierniewski J.:** The influence of the viewing geometry of bare rough soil surfaces on their spectral response in the visible and near-infrared range. Remote Sensing Environ., 127, 135-142, 1989.
3. **Cierniewski J., Baret F., Verbrugghe M., Jacquemoud S., Hanocq J.:** Geometrical modelling of soil bidirectional reflectance incorporating specular effects. Int. J. Remote Sensing, 7, 3691-3704, 1996.
4. **Cierniewski J., Courault D.:** Bidirectional reflectance of bare soil surfaces in the visible and near-infrared rang. Remote Sensing Rev., 7, 321-339, 1993.
5. **Cierniewski J., Verbrugghe M.:** A geometrical model of soil bidirectional reflectance in the visible and near-infrared range (in Polish). Fotointerpretacja w Geografii, 23, 37-51, 1993.
6. **Cierniewski J., Verbrugghe M.:** A geometrical model of soil bidirectional reflectance in the visible and near-infrared range. Proc. 6th Int. Measurements and Signatures in Remote Sensing, Val d'Isere, France, 635-642, 1994.
7. **Cierniewski, J., Verbrugghe, M.:** Influence of soil surface roughness on soil bidirectional reflectance. Int. J. Remote Sensing (in print).
8. **Cooper K.D., Smith J. A.:** A Monte Carlo reflectance model for soil surfaces with three-dimensional structure. IEEE Trans. Geosci. Remote Sensing, 1GE-23, 668-667, 1985.
9. **Deering D.W., Eack T.F., Otterman J.:** Bidirectional reflectances of selected desert surfaces and their three-parameter soil characterization. Agric. Forest Meteor., 1, 52, 71-93, 1990.
10. **Graetz R.D., Gentle M.R.:** A study of the relationship between reflectance characteristics in the Landsat wavebands and the composition and structure of an Australian semi-arid rangeland. Photogrammetric Engineering and Remote Sensing, 148, 1721-1736, 1982.

11. **Huete A.R.:** Soil and Sun angle interactions on partial canopy spectra. Int. J. Remote Sensing, 18: 1307-1317, 1987.

12. **Kimes D.S., Seller P.J.:** Inferring hemispherical reflectance of the Earth's surface for global energy budget from remotely sensed nadir or directional radiance values. Remote Sensing Environ., 118, 205-223, 1985.

13. **Milton E.J., Webb J.P.:** Ground radiometry and airborne multispectral survey of bare soils. Int. J. Remote Sensing, 18, 3-14, 1987.

14. **Norman, J. M., Welles, J. M., Walter, E. A.:** Contrast among bidirectional reflectance of leaves, canopies, and soils. IEEE Trans. Geosci. Remote Sensing, 1GE-23, 659-667, 1985.

15. **Ott W., Pfeiffer B., Quiel F.:** Directional reflectance properties determined by analysis of airborne multispectral scanner data and atmospheric correction. Remote Sensing Environ., 116, 47-54, 1984.

16. **Pech R.P., Graetz R.R., Davis A.W.:** Reflectance modelling and the derivation of vegetation indices for an Australian semi-arid shrubland. Int. J. Remote Sensing, 17, 389-403, 1986.

17. **Ranson K.J., Biehl L.L., Bauer M.E.:** Variation in spectral response of soybeans with respect to illumination, view and canopy geometry. Int. J. Remote Sensing, 16, 1827-1842, 198.